MEMO^2: MEthane goes MObile – MEasurements and MOdelling

Improved bottom-up European CH_4 emissions

Lead author

Hugo Denier van der Gon

TNO

Princetonlaan 6,

3584 CB Utrecht, The Netherlands;

Co-authors

Hossein Maazallahi (UU / TNO)

Barbara Szenasi (LSCE)

Thomas Röckmann (UU)

Felix Vogel (Env. Canada)

And MEMO^2 team

MEMO^2 contact

Telephone: +31 30 253 3167

Email: s.walter@uu.nl

Deliverable D3.2			
Delivery month Annex I	30		
Actual delivery month	48		
Lead participant: UU	WP: 3	Nature: report	Dissemination level: public
Version: 01			

This project has received funding from the European Union's Horizon 2020 research and innovation programme under the Marie Sklodowska-Curie grant agreement No 722479.

Table of contents

1. Executive Summary

The MEMO² project benefited strongly from concomitant societal and scientific developments and projects as regards detection and quantification of methane (CH_4) emissions from various sources and source areas. The idea behind the workflow, leading towards deliverable D3.2, was that the novel techniques deployed in MEMO² can facilitate a measurement-based emission assessment which can be compared against the traditional inventory guidebook approach of combining emission factors and activity data. The result would be an improved, more certain emission map. The greatest opportunity to apply this workflow opened through the United Nations - initiated study on CH_4 emission detection, quantification and attribution in cities, with special focus on leaks from the urban natural gas networks. MEMO² partners were able to take on key roles in this project and from our consortium we covered the following cities in Europe:

- Hamburg, Germany (Maazallahi et al., ACP, 2020)
- Utrecht, Netherlands (Maazallahi et al., ACP, 2020)
- Paris, France (Defratyka et al., Environmental Science and Technology, in press, 2021)
- Bucharest, Romania, (Fernandez et al, Atmospheric Environment, ready for submission)
- London, UK, (Fernandez et al., in preparation)
- Groningen, Netherlands (Vinkovic et al., in preparation)
- Katowice, Poland (Stanisavljević et al., in preparation)
- Swansea, UK, (Fernandez et al., in preparation)
- Birmingham, UK (Bakkaloglu et al., in preparation)

This MEMO² set represents 9 of the 13 cities (EU plus Toronto, Canada) that are presently evaluated as part of a synthesis study on CH_4 emissions from European cities. Since the MEMO² project strongly evolved in this direction, much of the work related to improved European CH_4 emissions is directed to the city scale. MEMO² partner organisations such as TNO and ECCC are closely involved in preparing the publication for synthesis, led by the former MEMO² PI Felix Vogel (now ECCC and leading the EU cities intercomparison study).

TNO and UU are presently providing the city scale inventory data, based on official country reporting and spatial distribution for this synthesis report. The availability of the measurement based (bottom-up) estimates and the currently used national scale top-down estimates allow us to evaluate differences and deliver a set of improved bottom-up estimates for city emissions in Europe.

A second part of inventory related work is associated with the international ROMEO measurement campaign (again, co-funded by UNEP), organised by the UU and carried out in 2019 by the MEMO² consortium. The evaluation of these data is in full swing, but will take longer than the operational period of MEMO², mainly due to delays associated with the COVID pandemic. The workflow as outlined above for the city data towards production of improved emissions for other emission categories cannot be completed as initially planned. For generating the improved emissions, we are in contact with the group that is responsible for the Romanian greenhouse gas inventory reports. This work will be continued and finished within the associated ROMEO project by the end of October 2021, and by this last beyond the lifetime of MEMO².

The improved bottom-up European CH_4 emissions will concentrate on city emissions. This will provide an excellent example how techniques and abilities developed under MEMO² can directly support policy relevant products like emission inventories. The information in this deliverable will be part of a peer-reviewed publication to ensure dissemination of the knowledge. As indicated above, emission estimates for the Romanian oil and gas production regions will be completed after MEMO² in the associated ROMEO project, but linked to and disseminated by MEMO².

Another important aspect for the inventory was source attribution using (new) source specific isotope measurements. The isotope specific emission maps made in MEMO² are presented in this deliverable. The results from the new measurements showed that the same source sector (especially oil and gas) can show very different isotopic signatures. Extrapolating new MEMO² data from limited locations to the entire European sector would be misleading but the potential of the method has been shown. Therefore, measurements of CH_4 and its isotopologues in more countries and locations are needed to gain more knowledge on CH_4 emissions in Europe and to improve CH_4 emission maps and isotopologue maps with as small uncertainties as possible.

2. Introduction

2.1 Background

Emission inventories are typically developed by using a bottom-up approach at the national scale, i.e. combining available national statistics on fuel combustion, industrial production, etc. with the most appropriate emission factors. For a detailed description on how emission inventories are constructed we refer to EEA[1] and IPCC[2]. This approach results in total emissions by sources or source sectors, but without a spatial distribution within the country.

For a good understanding of environmental problems, not only the magnitude of the sources but also their location is important. The spatially distributed emissions need to cover the complete (national or regional) domain, and describing the emissions in a consistent way, i.e. in all countries the same sources should be included, and these sources should be assessed as accurately and consistently as possible.

Proxy maps can be used to spatially distribute the national total emissions. These proxies provide the mapping of the emissions of a certain pollutant to the grid for a given sector and year. For each country, pollutant, sector, and year the most appropriate proxy needs to be selected. Examples of possible proxy maps are e.g. road networks, land use maps, or urban population density.

Generally speaking for anthropogenic emission sources, population density is the default proxy map. This implies that if it is not known where emissions exactly occur they are distributed using population density information (maps).

An example of an emission map for CH_4 is given in Fig. 1. This map is composed of various emission sources like landfills, wastewater treatment plants, gas production etc. Some of these are distributed by a unique map, others by a default proxy map.

Emissions from natural gas distribution networks (NGDNs) are typically distributed using population density because information on the exact location of leaks is scarce. This implies that CH_4 emissions in European cities are not well known, and we assume an average distribution proportional to population density. In order to get better and more accurate data, extensive campaigns must be carried out to collect the necessary observational data.

Only few studies have estimated urban CH_4 fluxes using eddy covariance measurements (Gioli et al., 2012; Helfter et al., 2016), airborne mass balance approaches (O'Shea et al., 2014) and the Radon-222 flux and mixing layer height techniques (Zimnoch et al., 2019). Gioli et al. (2012) showed that about 85 % of CH_4 emissions in Florence, Italy originated from natural gas leaks.

[1] https://www.eea.europa.eu/themes/air/air-pollution-sources-1/emep-eea-air-pollutant-emission-inventory-guidebook/emep
[2] https://www.ipcc.ch/report/2006-ipcc-guidelines-for-national-greenhouse-gas-inventories/

Helfter et al. (2016) estimated CH_4 emissions of (72 ± 3) t km^{-2} yr^{-1} in London, UK mainly from sewer system and NGDN leaks, which is twice as much as reported in the London Atmospheric Emissions Inventory. O'Shea et al. (2014) also showed that CH_4 emissions in greater London is about 3.4 times larger than the report from UK National Atmospheric Emission Inventory. Zimnoch et al. (2019) estimated CH_4 emissions of $(6.2 \pm 0.4) \times 10^6$ m^3 $year^{-1}$ for Krakow, Poland, based on data for the period of 2005 to 2008 and concluded that leaks from NGDNs are the main emission source in Krakow, based on carbon isotopic signature of CH_4. Chen et al. (2020) also showed that incomplete combustion or loss from temporarily installed natural gas appliances during big festivals can be the major source of CH_4 emissions from such events, while these emissions have not been included in inventory reports for urban emissions.

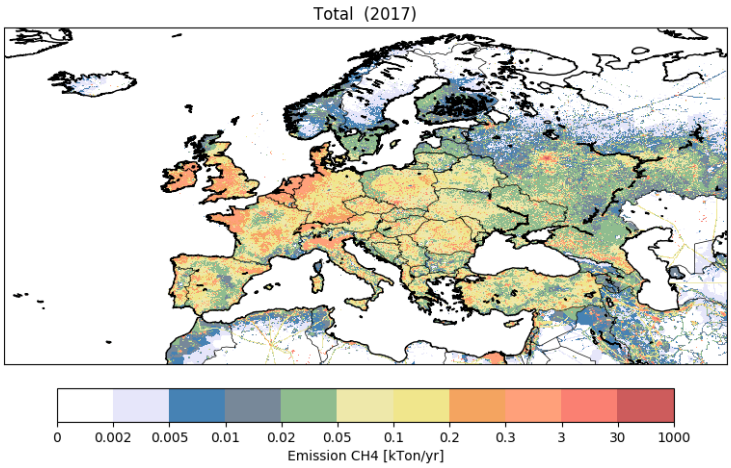

Fig. 1: Total European CH_4 emission (kt/yr/gridcell) according to the TNO-GHGco emission inventory for the year 2017.

Regarding CH_4 emissions from NGDNs, a number of intensive CH_4 surveys with novel mobile high precision laser-based gas analysers in US cities have recently revealed the widespread presence of leak indications (LIs: CH_4 enhancements of more than 10 % above background level) with a wide range of magnitudes (Weller et al., 2020; Weller et al., 2018; von Fischer et al., 2017; Chamberlain et al., 2016; Hopkins et al., 2016; Jackson et al., 2014; Phillips et al., 2013). The number and severity of natural gas leaks appears to depend on pipeline material and age, local environmental conditions, pipeline maintenance and replacement programs (von Fischer et al., 2017; Gallagher et al., 2015; Hendrick et al., 2016). For example, NGDNs in older cities with a larger fraction of cast iron or bare steel pipes showed more frequent leaks than NGDNs that use the newer plastic pipes. The data on CH_4 leak indications from distribution systems in cities have provided valuable data for emission reduction in the US cities which allows local distribution companies (LDCs) who are in charge of NGDN to quickly fix leaks and allocate resources efficiently (Weller et al., 2018, von Fischer et al., 2017, Lamb et al., 2016; McKain et al., 2015).

2.2 Scope of the deliverable

This deliverable focusses on the urban CH_4 emissions as measured using new innovative mobile CH_4 measurement techniques deployed by MEMO². Thus, the contribution to improved bottom-up European CH_4 emissions will concentrate on city (urban) emissions. This provides an excellent example how techniques and abilities developed under MEMO² can directly support policy relevant products like emission inventories. The information in this deliverable will be and in some cases is already part of a peer-reviewed publication to ensure dissemination of the knowledge.

3. City inventories for CH_4 emission from natural gas distribution

3.1 Introduction

Mobile campaigns of CH_4 emissions in cities have been previously executed in the US. Results demonstrate that emissions from various cities can highly differ although the cites are being located in the same country (Fig. 2). This implies that the default proxy of population density to distribute CH_4 emission from gas distribution networks is most likely not suitable. This hypothesis has been investigated by MEMO² in more detail for European cities.

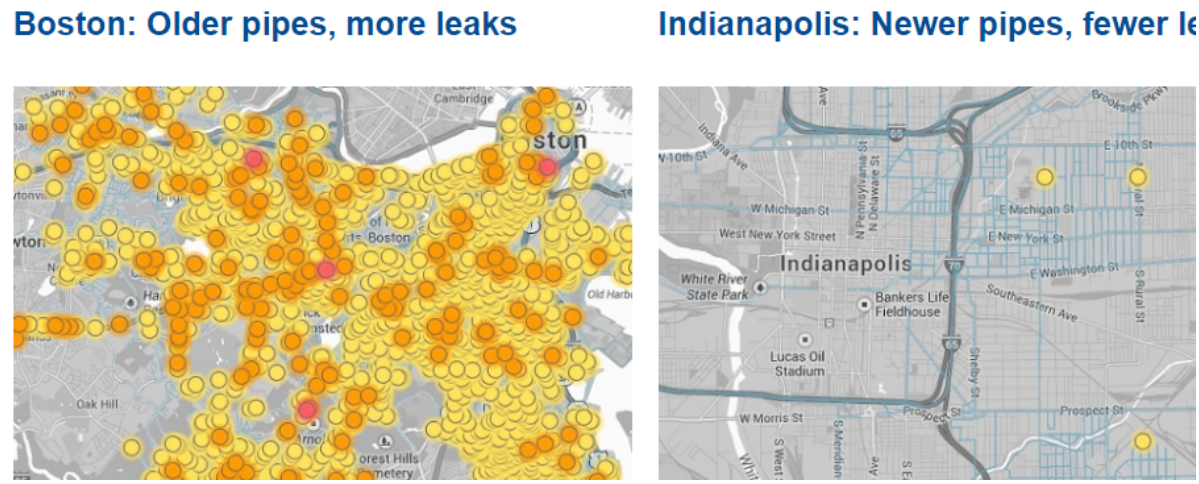

Fig. 2: Example maps from the US cities project showing to extreme differences in leak density (source: https://www.edf.org/climate/methanemaps)

3.2 Mobile measurements in European cities

3.2.1 General Approach

Mobile surveys were carried out in several European cities with online analysers. Emissions were derived using a quantification approach initially introduced in von Fischer et al. (2017) and improved in Weller et al. (2019).

The algorithm was designed to quantify CH_4 emissions from ground-level emission release locations within 5 - 40 m from the measurement (von Fischer et al., 2017), and it has been demonstrated that the algorithm adequately estimates the majority of those emissions from a city (Weller et al., 2018). Fig. 3 shows the steps taken to map, quantify, and evaluate CH_4 emission in Utrecht, Hamburg and Bucharest.

Weller et al., (2019) established an empirical equation to convert concentration elevations observed with a Picarro G2301 instrument in a moving vehicle in urban environments into emission rates based on a large number of controlled release experiments in various environments (Eq. (1)).

$$\mathrm{Ln}(C) = -0.988 + 0.817 * \mathrm{Ln}(Q) \qquad (1)$$

where C represents CH_4 enhancements above the background in ppm and Q is the emission rate in L min^{-1}. Weller et al., (2019) also characterized the limitations and associated errors of this equation.

The spatial extent of individual leak indications (LIs) was estimated as the distance between the location where the CH_4 mole fraction exceeded the background by more than 10 % (≈ 0.200 ppm; as used in von Fischer et al. (2017) and Weller et al. (2019)) to the location where it fell below this threshold level again. In a continuous measurement survey on a single day, consecutive CH_4 enhancements above background observed within 5 seconds were aggregated and the location of the emission source was estimated based on the weighted averaging of coordinates (Eq. (2)).

$$(\text{lon, lat}) = \frac{\sum_{i=1}^{n} w_i * (lon_i, lat_i)}{\sum_{i=1}^{n} w_i} \qquad (2)$$

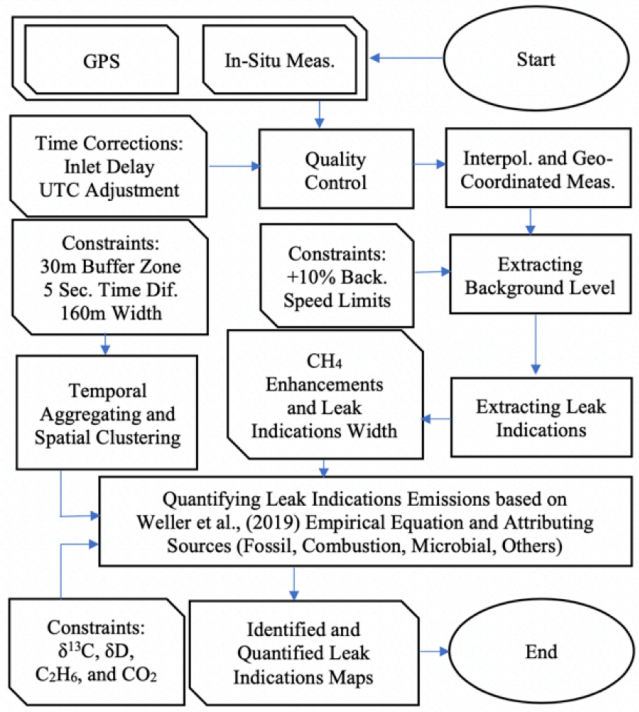

Fig. 3: Flowchart of evaluating CH4 emissions in urban area

LIs observed on different days at similar locations were clustered and interpreted as a point source when circles of 30 m radius around the centre locations overlapped, similar to Weller et al., (2019). The natural logarithm of maximum CH_4 enhancement from each transect for each cluster were then averaged and used to quantify emission related to each cluster. The representative location of LI for each cluster was assigned by using weighted average of the geographical coordinates of the LIs within that cluster (Eq. (2) from Weller et al. (2019)), where w_i is CH_4 enhancement of each LI.

The quantification algorithm was compared to the original one from Colorado State University, showing an excellent agreement (Fig. 4).

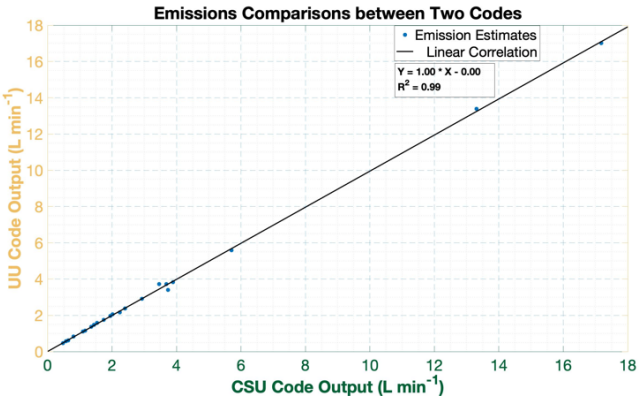

Fig. 4: Comparison of codes output developed in Utrecht University (UU) with results from the code of Colorado State University (CSU)

The emission rate per km of road covered during our measurements was scaled up to the city scale using the ratio of total road length within the study area boundaries derived from OSM to the length of streets covered, and converted to a per-capita emission using the population in the study areas based on LandScan data (Bright et al., 2000). Note that in this up-scaling practice, emission quantified from facilities were excluded.

To account for the emission uncertainty, similar to Weller et al. (2018) for the US city studies, we used a non-parametric bootstrap technique to account for the uncertainty of total CH_4 emissions from all LIs in each city. Whereas leak rate estimates of individual LIs can have large errors (Fig. 4 in Weller et al. (2019)), the uncertainty associated with total city estimates are more precise.

3.2.2 Utrecht and Hamburg

3.2.2.1 General overview

The distribution of CH_4 LIs across the cities of Utrecht and Hamburg is shown in Fig. 5. As shown in Table 1, a total of 145 significant LIs were detected in Hamburg and 81 in Utrecht; these LIs cover all three LI categories. Two LIs in Hamburg and one LI in Utrecht fall in the high emission category; the highest LI detected in Utrecht and Hamburg corresponded to emission rates of ≈ 100 L min^{-1} and ≈ 70 L min^{-1}, respectively. Six LIs in Utrecht and 16 LIs in Hamburg fall in the middle emission category, and 127 LIs in Hamburg and 74 LIs in Utrecht fall in the low emission category. The distribution of emissions over the three categories is also similar between the two cities, with roughly one third of the emissions originating from each category, but the number of LIs in each category is different. The contribution of LIs in the high emission category is about a third of the total observed emissions (35 % in Utrecht is (1 LI) and in 30 % in Hamburg (2 LIs)).

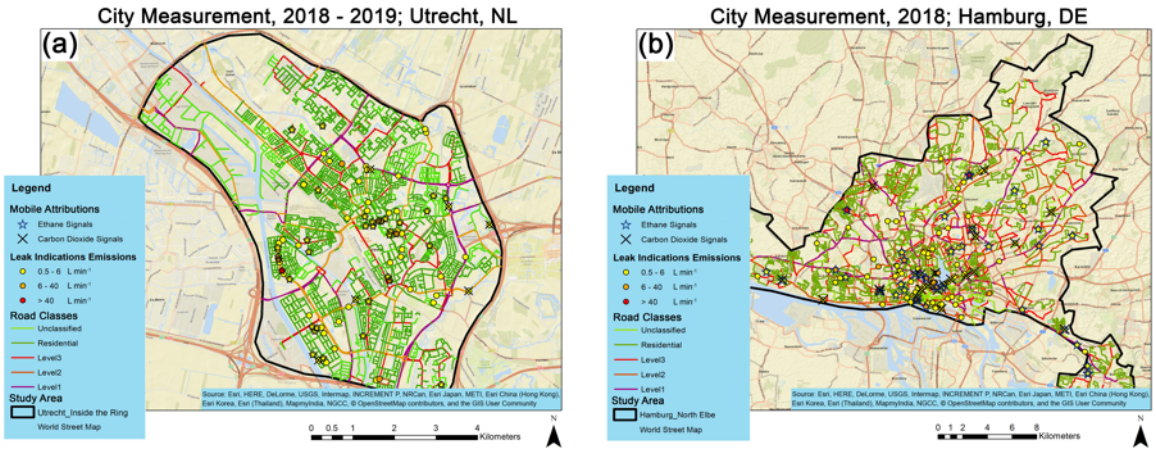

Fig. 5: Distribution of CH_4 emission locations across Utrecht (a) and Hamburg (b)

Table 1 summarizes for the example cities of Utrecht and Hamburg how the derived methane emission rates were converted to emission factors that are the basis of updated city scale emission estimates, including attribution of emission to different categories. More details are provided in Maazallahi et al. (2020).

Table 1: Conversion of observed emission rates to emission factors and total-city emissions of methane, from Maazallahi et al. (2020).

Study Area			Utrecht (inside the Ring)	Hamburg (North Elbe)
≈ km street driven		Total km driven	1,000 km	1,800 km
		Driven once	220 km	900 km
		Driven more than once	780 km	900 km
≈ km street covered		Total km covered	450 km	1,200 km
		covered once	230 km	900 km
		covered more than once	220 km	300 km
LIs and emissions		Total number	81 LIs	145 LIs
		LI density	5.6 km covered LI^{-1}	8.4 km covered LI^{-1}
		Total emission rate	290 L min^{-1}	490 L min^{-1}
		Average emission rate per LI	3.6 L min^{-1} LI^{-1}	3.4 L min^{-1} LI^{-1}
		Total emission rate per year	107 t yr^{-1}	180 t yr^{-1}
LIs visited	Once	Number	16 LIs	45 LIs
		Emissions	26 L min^{-1}	68 L min^{-1}
		Average emission rate per LI	1.6 L min^{-1} LI^{-1}	1.5 L min^{-1} LI^{-1}
		Number	65 LIs	100 LIs

	More than once	Emissions		264 L min^{-1}	423 L min^{-1}
		Average emission rate per LI		4.1 L min^{-1} LI^{-1}	4.2 L min^{-1} LI^{-1}
Total LIs categorized based on von Fischer et al. (2017) categories	High (>40 L min^{-1})	Number		1 LI	2 LIs
		Emissions		102 L min^{-1}	145 L min^{-1}
		Average emission rate per LI		101.5 (L min^{-1} LI^{-1})	72.4 L min^{-1} LI^{-1}
		% of emissions		35 % of total emissions	30 % of total emissions
	Medium (6-40 L min^{-1})	Number		6 LIs	16 LIs
		Emissions		84 L min^{-1}	176 L min^{-1}
		Average emission rate per LI		14.0 L min^{-1} LI^{-1}	11 L min^{-1} LI^{-1}
		% of emissions		30 % of total emissions	36 % of total emissions
	Low (0.5-6 L min^{-1})	Number		74 LIs	127 LIs
		Emissions		105 L min^{-1}	169 L min^{-1}
		Average emission rate per LI		1.4 L min^{-1} LI^{-1}	1.3 L min^{-1} LI^{-1}
		% of emissions		36 % of total emissions	35 % of total emissions
Total LIs categorized based on OSM road classes	Level 1	Number		6 LIs	29 LIs
		Emissions		5 L min^{-1}	68 L min^{-1}
		Average emission rate per LI		0.76 L min^{-1} LI^{-1}	2.3 L min^{-1} LI^{-1}
	Level 2	Number		16 LIs	34 LIs
		Emissions		145 L min^{-1}	99 L min^{-1}
		Average emission rate per LI		9.0 L min^{-1} LI^{-1}	2.9 L min^{-1} LI^{-1}
	Level 3	Number		3 LIs	23 LIs
		Emissions		10 L min^{-1}	43 L min^{-1}
		Average emission rate per LI		3.4 L min^{-1} LI^{-1}	1.9 L min^{-1} LI^{-1}
	Residential	Number		45 LIs	52 LIs
		Emissions		93 L min^{-1}	274 L min^{-1}
		Average emission rate per LI		2.1 L min^{-1} LI^{-1}	5.3 L min^{-1} LI^{-1}
	Unclassified	Number		11 LIs	7 LIs
		Emissions		38 L min^{-1}	6 L min^{-1}
		Average emission rate per LI		3.4 L min^{-1} LI^{-1}	0.8 L min^{-1} LI^{-1}
Attribution	C_2:C_1 ratio analysis	Fossil (Inc. combustion)	% of emissions	93 % of total emissions	64 % of total emissions
			% of LIs	69 % of LIs	33 % of LIs
		Microbial	% of emissions	6 % of total emissions	25 % of total emissions
			% of LIs	10 % of LIs	20 % of LIs
		Unclassified	% of emissions	1 % of total emissions	11 % of total emissions
			% of LIs	21 % of LIs	47 % of LIs
	$\delta^{13}C$ and δD analysis	Fossil	% of emissions	----------	79 % of total emissions
			% of LIs	----------	38 % of LIs
		Microbial	% of emissions	----------	20 % of total emissions
			% of LIs	----------	54 % of LIs
		Other	% of emissions	----------	1 % of total emissions
			% of LIs	----------	8 % of LIs (Pyrogenic)
	CH_4:CO_2 ratio analysis	Combustion	% of emissions	2 %	10 %
			% of LIs	7 %	17 %
		Other	% of emissions	98 %	90 %
			% of LIs	93 %	83 %
	C_2:C_1 ratio, CH_4:CO_2 ratio, and $\delta^{13}C$ - δD	Fossil	% of emissions	73 %	48 %
			% of LIs	43 %	31 %
		Combustion	% of emissions	2 %	10 %
			% of LIs	7 %	17 %
		Microbial	% of emissions	8 %	35 %
			% of LIs	4 %	33 %
			% of emissions	16 %	7 %

	anal-yses	Unclas-sified	% of LIs	46 %	19%
Average emission rate per km driven				0.29 L min^{-1} km^{-1}	0.27 L min^{-1} km^{-1}
km driven / total LIs				12.5 km LI^{-1}	12.36 km LI^{-1}
Emission factors to scale-up emissions per km covered				0.64 L min^{-1} km^{-1}	0.40 L min^{-1} km^{-1}
km covered per LIs			km covered / total LIs	5.6 km LI^{-1}	8.4 km LI^{-1}
			km covered / red LIs	454.8 km LI^{-1}	611.4 km LI^{-1}
			km covered / orange LIs	75.8 km LI^{-1}	76.4 km LI^{-1}
			km covered / yellow LIs	6.1 km LI^{-1}	9.6 km LI^{-1}
km road from OSM (≈ km pipeline)				≈ 650 km	≈ 3000 km
Up-scaled methane emissions to total roads				420 L min^{-1} (≈150 t yr^{-1})	1,200 L min^{-1} (≈440 t yr^{-1})
Bootstrap emission rate estimate and error				420 ± 120 L min^{-1}	1,200 ± 170 L min^{-1}
Population in study area				≈ 0.28 million	≈ 1.45 million
Average LIs emissions per capita (kg yr^{-1} $capita^{-1}$)				0.54 ± 0.15	0.31 ± 0.04
Yearly natural gas consumption				≈ 0.16 bcm yr^{-1}	≈ 0.75 bcm yr^{-1}
Fossil emission factors	C_2:C_1 ratio attribution analysis		Average emission rate per km gas pipeline	0.60 ± 0.2 L min^{-1} km^{-1}	0.26 ± 0.04 L min^{-1} km^{-1}
			Average emission rates per capita	0.50 ± 0.14 kg yr^{-1} $capita^{-1}$	0.20 ± 0.03 kg yr^{-1} $capita^{-1}$
	$\delta^{13}C$ and δD attribution analysis		Average emission rates per km gas pipeline	----------	0.32 ± 0.05 L min^{-1} km^{-1}
			Average emission rates per capita	----------	0.25 ± 0.04 kg yr^{-1} $capita^{-1}$
	C_2:C_1 ratio, CH_4:CO_2 ratio, and $\delta^{13}C$ - δD analyses		Average emission rates per km gas pipeline	0.47 ± 0.14 L min^{-1} km^{-1}	0.19 ± 0.03 L min^{-1} km^{-1}
			Average emission rates per capita	0.39 ± 0.11 kg yr^{-1} $capita^{-1}$	0.15 ± 0.02 kg yr^{-1} $capita^{-1}$
			Average emission rates / yearly consumption	0.10 – 0.12 %	0.04 – 0.07 %

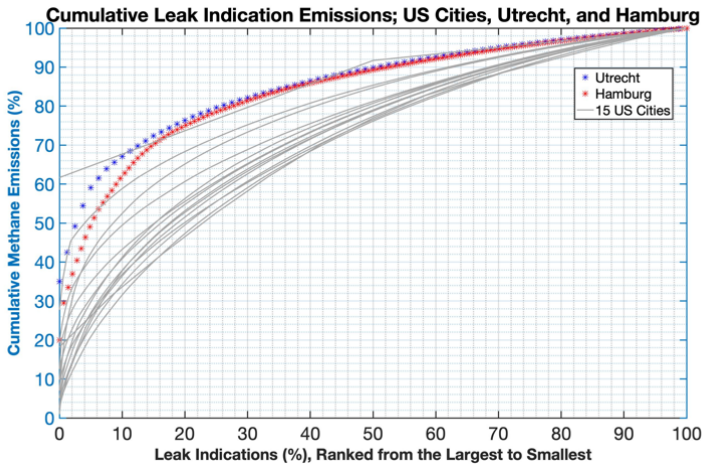

Fig. 6: Cumulative plot of CH_4 emissions in US cities and Utrecht and Hamburg

In Fig. 6, we compare cumulative CH_4 emissions for Utrecht and Hamburg to numerous US cities (Weller et al., 2019). After ranking the LIs from largest to smallest, it becomes evident that the largest 5 % of the LIs account for about 60 % of emissions in Utrecht, and 50 % of the emissions in Hamburg.

The observed total emission rates observed on roads in the two cities are relatively similar when normalized by the total amount of km covered, 0.64 L min^{-1} km^{-1} for Utrecht and 0.4 L min^{-1} km^{-1} for Hamburg (Table 1). Using these two emission factors, the observed emission rates (≈ 110 t yr^{-1} in Utrecht and ≈ 180 t yr^{-1} in Hamburg) were up-scaled to the entire road network in the two cities, ≈ 650 km in Utrecht and ≈ 3,000 km in Hamburg. This includes the implicit assumption that the pipeline network is similar to the street network.

Total up-scaled emission rates based on mobile measurements on roads in urban environment before considering attribution analysis over LI locations are 150 t yr^{-1} and 440 t yr^{-1} across the study areas of Utrecht and Hamburg respectively. Distributing the calculated emission rates over the population in the city areas yields emission rates of 0.54 ± 0.15 kg yr^{-1} $capita^{-1}$ for Utrecht and 0.31 ± 0.04 kg yr^{-1} $capita^{-1}$ for Hamburg (Fig. 7).

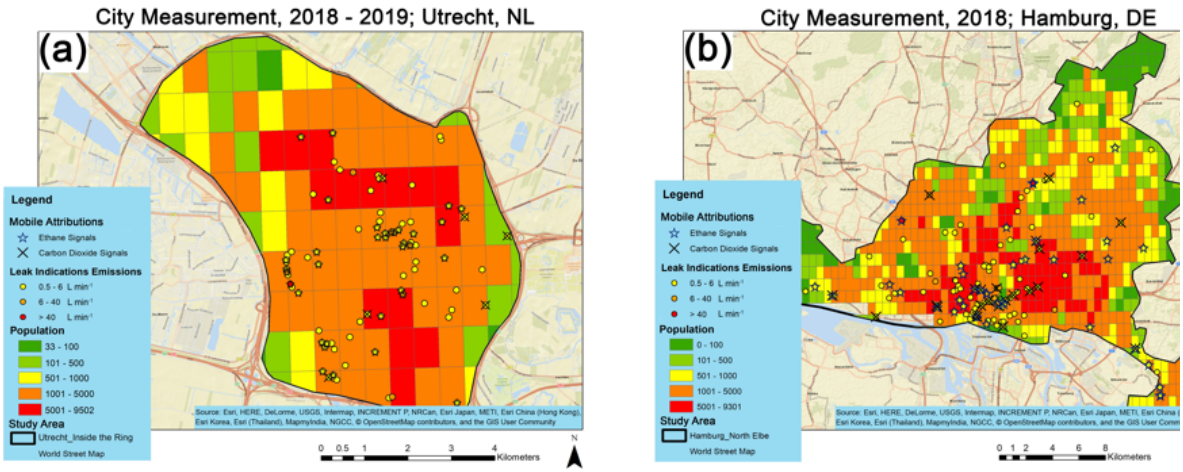

Fig. 7: Maps of population distribution in combination with spread of CH_4 emission locations in Utrecht (a) and Hamburg (b)

3.2.2.2 Comparison to national inventory reports

In the national inventory reports, total upscaled emissions from NGDNs are based on sets of emission factors for different pipeline materials (e.g., grey cast iron, steel, or plastic) at different pressures (e.g., < = 200 mbar or > 200 mbar). The reported emission factors are based on IPCC tier 3 approach (Buendia et al., 2019). However, emission estimates do not exist for individual cities including Utrecht and Hamburg. Also, it is not possible to calculate a robust city-level estimate using the nationally reported emission factors because there is no publicly available associated activity data, i.e., pipeline materials and lengths for each material, at the level of individual cities. As a result, a robust direct comparison between nationally reported emissions and our measurements, akin to a recent study in the United States (Weller et al., 2020), is currently not possible. The following juxtaposition of our estimates and national inventory downscaling to city-level is therefore provided primarily as illustration of the data gaps rather than a scientific comparison. In Utrecht, we attributed 70 – 90 % of the mobile measurement inferred emissions of ≈ 150 t yr^{-1} to the NGDN, thus 105 – 135 t yr^{-1}.

Related to the measurements in Utrecht, the Netherlands National Institute for Public Health and the Environment (RIVM) inventory report derived an average NGDN emission factor of ≈ 110 kg km^{-1} yr^{-1} using 65 leak measurements from different pipeline materials and pressures in 2013. This weighted average ranged from a maximum of 230 kg km^{-1} yr^{-1} for grey cast iron pipelines to a minimum of 40 kg km^{-1} yr^{-1} for pipelines of other materials with overpressures <= 200 mbar (for details, see P. 130 in Peek et al. (2019)). This results in an average CH_4 emissions of ≈ 70 t yr^{-1} (min = 30 t yr^{-1} and max = 150 t yr^{-1}) for the study area of Utrecht, assuming ≈ 650 km of pipelines inside the ring, and further assuming that Utrecht's NGDN is representative of the national reported average (see qualifiers above). The average emissions for the Utrecht study, based on emissions factors reported for the Netherlands, is smaller by a factor of 1.5 - 2 compared to the emissions derived here. The variability factor of 5, from the reported emission (resulting from the variability in pipeline materials) highlights the need for city-level specific activity data for a robust comparison.

In Hamburg, 50 – 80 % of the upscaled emissions of 440 t yr^{-1} (220 – 350 t yr^{-1}), can be attributed to the emission from the NGDN. The national inventory from the Federal Environment Agency (UBA) in Germany, reports an average CH_4 emission factor for NGDN from low pressure pipelines as ≈ 290 kg km^{-1} yr^{-1} (max = 445 kg km^{-1} yr^{-1} (grey cast iron) and min = 51 kg km^{-1} yr^{-1} (plastic)) based on measurements from the 1990s (Table 169 in Federal Environment Agency (2019)). Assuming ≈ 3000 km of pipelines in the targeted region, and further assuming that Hamburg's NGDN is representative of the national reported average (see qualifiers above), results in an estimated NGDN CH_4 emissions average of ≈ 870 t yr^{-1} (min = 155 t yr^{-1} and max = 1350 t yr^{-1}).

While this study's estimate (220 – 350 t yr^{-1}) falls in the lower end of this range, the reported emissions variability factor of 9 (resulting from the variability in pipeline materials) highlights again the need for city-level specific activity data for a robust comparison. To put the national inventory comparison into perspective, it should be noted that GasNetz Hamburg detected and fixed leaks at 20 % of the fossil LIs in this study, which accounted for 50 % of emissions.

In Utrecht and Hamburg, the natural gas consumption data for our target areas were retrieved through communications with LDCs. In the Utrecht and Hamburg study areas, natural gas consumption is 0.16 bcm yr^{-1} (STEDIN, personal communication) and 0.75 bcm yr^{-1} (GasNetz Hamburg, personal communication) respectively. The estimated emissions from NGDNs in our study is between 0.10 – 0.12 % in Utrecht and between 0.04 – 0.07 % in Hamburg of total the annual natural gas consumptions in the same area. In the US, where the majority of natural gas consumption is from residential and commercial sectors, Weller et al. (2020) reported emissions of 0.69 Tg $year^{-1}$ (0.25 - 1.23 with 95 % confidence interval), with a sum of ≈ 170 Tg $year^{-1}$ (U.S. EIA, 2019), showing 0.4 % (0.15 % - 0.7 %) loss from NGDNs. The US NGDNs loss is about four times larger than our reported loss in Utrecht, and is about ten times larger than the loss for Hamburg. Considering the population of Utrecht (≈ 0.28 million) and Hamburg (≈ 1.45 million), the natural gas consumption densities in these study areas are ≈ 570 m^3 $capita^{-1}$ yr^{-1} and ≈ 520 m^3 $capita^{-1}$ yr^{-1}, where in the US (population ≈ 330 million (US Census Bureau, 2020)) the density is about ≈ 730 m^3 $capita^{-1}$ yr^{-1}. This shows that annual natural gas consumption per capita in the US is about 30 % and 40 % higher than in Utrecht and Hamburg respectively. The emission per km of pipeline in Utrecht is between 0.45 – 0.5 L min^{-1} km^{-1} and in Hamburg is between 0.2 – 0.32 L min^{-1} km^{-1}. In the US, based on 2,086,000 km km of local NGDN pipeline (Weller et al., 2020), this emission factor will be between 0.32 – 1.57 L min^{-1} km^{-1}. This shows higher emissions per km pipeline in the countrywide studies of US compared to just two European cities of Utrecht and Hamburg (see qualifiers above). This can be partly explained by pipeline material, maintenance protocols, and higher natural gas consumption in the US. However, the substantial variability in emission rates across US cities, as wells as the annual variability of gas consumption over the year, again restricts a direct comparison of two cities with a national average measured over multiple years.

Normalized LIs emissions per capita in Utrecht (0.54 ± 0.15 kg yr^{-1} $capita^{-1}$) are almost double the emission factor in Hamburg (0.31 ± 0.04 kg yr^{-1} $capita^{-1}$). This metric may be useful to compare cities, assuming that the emission quantification method is equally effective for different cities. CH_4 emissions can vary among different cities, depending on the age, management and material of NGDNs, and/or the management of local sewer systems. In our study, we only surveyed two cities, and the above number may not be adequate for extrapolation to the country scale (McKain et al., 2015).

3.2.3 Bucharest - Leak indications and attribution

Locations and the spatial distribution of the accepted clusters of CH_4 enhancements in Bucharest are seen in Fig. 8. It should be remembered that these locations represent CH_4 emissions from any source, not just gas pipelines. From the distance covered in Bucharest, 2482 CH_4 enhancement indicators were identified, where the maximum CH_4 excess was 38 ppm (mean = (1 ± 0.1) ppm s.e.) (Table 1). Of these

locations, the maximum inferred emission rate was 45 L min^{-1} (mean = of (2 ± 0.1) L min^{-1} s.e.; n = 969). Dividing the number of enhancement locations in Bucharest by the road coverage determines a CH_4 enhancement density of 0.7 (enhancements per km covered) (Table 1). Using the same distance as a proxy for pipeline length, the final emission factor calculated was 1.6 L km^{-1} min^{-1}.

In Ploieşti, 87 CH_4 enhancements indicators were detected within the 233 km of road covered, that account for 76 CH_4 enhancement locations (Table 1). Similar to Bucharest, Ploieşti has a maximum CH_4 excess of 38 ppm ((1 ± 1) ppm s.e; n = 76). Ploieşti's maximum emission rate found was 15 L min^{-1} (mean = (2 ± 0.3) L min^{-1} s.e.). Taking the total number of CH_4 enhancement indicators to the total road distance covered, calculates a CH_4 enhancement density of 0.4 (enhancements km^{-1}) and an emission factor of 0.6 L km^{-1} min^{-1}.

Fig. 8: Methane emission rate categories of Bucharest (left) and Ploieşti (right). Bucharest has 969 CH_4 emission localities that were identified through clustering a total of 2482 CH_4 indicators. The major Drumul Potcoavei leaks (northeast of the Bucharest boundary) include 7 emission locations which were clustered from 89 CH_4 indicators. Ploieşti includes 76 enhancement locations, clustered from 87 CH_4 indicators. Within the Bucharest border (solid blue line), the max emission was 291 L min^{-1} and 290 L min^{-1} for Ploieşti. Magnitude categories defined in von Fisher et al., 2017. The corresponding data are summarized in Table 1.

Based on the evaluation of the C_2:C_1 dataset, the LIs observed in Bucharest are 63 % biogenic (wastewater), 33 % identify as thermogenic (fossil fuel), and 4 % indicate other/pyrogenic origins (Table 2). Similar fractions can be derived from the isotope analysis, supporting the reliability of this attribution. Thus, overall, Bucharest C_2:C_1 ratios, within the city boundary, are dominantly more biogenic, and are most likely from wastewater.

Table 2: Source tracers of locations of enhanced methane. Source categories are defined by δ^2H_{CH4} and C_2:C_1. Biogenic (< -270 ‰, < 0.005) sources are assumed to be from wastewater and thermogenic (≥ -270 ‰; ≥ 0.005 to < 0.090) sources are assumed to be from the natural gas distribution system. $\delta^{13}C_{CH4}$ source apportionment is not utilized because known signatures overlap between biogenic (-58 to -49 ‰) and thermogenic (-60 to -43 ‰).

Source tracer		Biogenic (wastewater)	Thermogenic (fossil fuel)	Other (Pyrogenic)
δ^2H (‰)	n	31	24	-
	Percent	58 %	42 %	-
C_2:C_1	n	70	37	4
	Percent	63 %	33 %	4 %

3.2.4 Paris - Leak indications and attribution

In the Paris city surveys that covered 500 km of streets, 90 leaks were detected (Fig. 9) and an origin of 27 leak indications was identified. Out of the latter 27, 15 are attributed to the natural gas network, 8 to sewage, and 4 to furnaces. Thus, 66 % of leak indications in Paris come from natural gas leaks and 34 % from sewage network. This distribution of source categories is propagated to the 63 leaks of unknown origin and 41 additional leaks are considered as coming from gas leaks and 22 as sewage network leaks (Fig 9b).

Using equation (1), we calculated the emission rate. For the fifteen determined natural gas distribution leak indications, the mean estimated emission rate is equal to 1.4 L/min (range 0.5 – 3.87 L/min) for individual leak indication. These natural gas leaks are categorized as small leaks (< 6 L/min), according to the categorization proposed by von Fischer et al.[7] For the sewage sector, the mean estimated emission rate for an individual leak indication is equal to 2.2 L/min (0.7 to 6.5 L/min). In this case, 7 leak indications are within the small category and one leak indication is within the medium category. For the furnace sector, the mean emission rate for an individual leak indication is equal to 3.5 L/min (0.7 to 5.9 L/min). The remaining 63 leak indications have a mean estimated emission rate equal to 1.4 L/min (0.5 – 10.5 L/min), where only one is categorized as a medium, which reached 10.5 L/min. Thus, in this group, the emission rates for individual leaks are skewed for lower emissions, with median values equal to 0.8 L/min.

Overall, for 500 unique km, the accumulated emission rate is equal to 140 L/min, where the gas sector contributes 56 % under our attribution assumption (Fig. 9b). The sewage sector and furnace category respectively contribute to 34 % and 10% of the accumulated rate. After upscaling this value to all kilometres of road in Paris and suburbs, the accumulated CH_4 emission rate of sources detectable from the ground is estimated to be equal to 500 L/min (190 t/yr). Such a simple extrapolation assumes a reasonable homogeneity of the leak distribution regarding the fraction of the total kilometres sampled during our surveys. Thus, in Paris at the street-level, 56 % of total CH_4 emissions come from leaks in natural gas distribution network, 34 % from leaks in sewage network and 10 % from furnaces leaking emissions. Looking only for the leaks in the natural gas distribution network, the natural gas leak indication rate (gas leak indications/ unique kilometres) is equal to 0.11 km^{-1}.

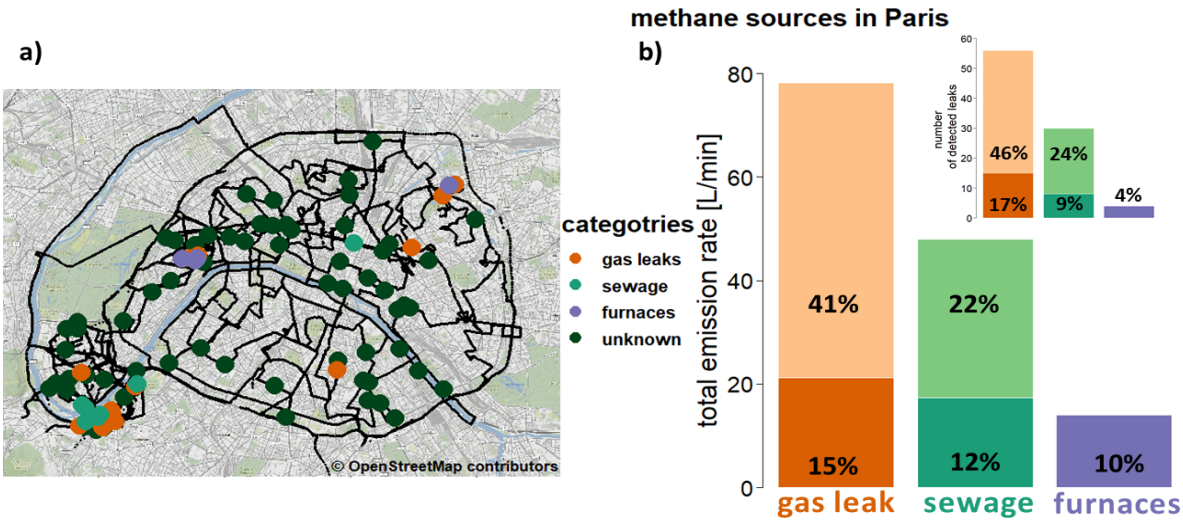

Fig. 9: CH_4 leak indication categories detected in the Paris area. a) Map of the surveyed area with positions of the detected sources. b) Distribution of the emission of the leak indication categories in the Paris area, inner figure: number of detected leaks. Paler colours represented unknown leaks attributed to gas leaks (orange) or sewage (green), based on the percent of defined leak indication. Base map provided by OpenStreetMap.

3.3 Summary of city inventory information for gas distribution

In order to derive improved emission factors for urban CH_4 emissions, the MEMO² consortium is heavily contributing to a synthesis publication with CH_4 emission measurements in numerous European cities, carried out in collaboration with the UNEP CCAC cities project with a strong contribution from MEMO² participants. TNO and UU have compiled the necessary inventory information shown in Table 3 that is currently under scientific evaluation by the cities consortium. Emission rates estimated according to CRF and Marcogaz can be different, up to a factor 4 (both smaller or larger), as can be seen in the last column of Table 3.

Table 3: Inventory information on CH_4 emission from natural gas distribution at the national scale and downscaled estimates in urban areas for nine European cities. (Note that is not representing the entire city population of the cities but only covers the part that was subject to MEMO² mobile campaigns).

		National scale			City scale				
City	**Coun-try (ISO3)**	**Marco-gaz 2018 estimate CH4 emis-sion (ton)**	**Country CH4 emis-sions NatGas distribu-tion 1B2b5, 2018 (ton)**	**Total country population**	**Country population in (urban) city area**	**Share of country popula-tion in city area (%)**	**CH_4 emis-sions urban city area (ton) - CRF**	**CH_4 emis-sions urban area (ton) - Marco-Gaz**	MG/CRF
Hamburg	DEU	92,175	86,965	80,854,418	1,286,862	1.6%	1,384	1,467	106%
Utrecht	NLD	21,987	5,556	16,923,311	246,766	1.5%	81	321	396%
Paris	FRA	33,069	23,341	64,444,919	2,989,176	4.6%	1,083	1,534	142%
Bucharest	ROU	3,097	12,974	21,666,350	1,230,817	5.7%	737	176	24%
London	GBR	57,374	136,243	64,088,222	5,298,179	8.3%	11,263	4,743	42%
Groningen	NLD	21,987	5,556	16,923,311	185,367	1.1%	61	241	396%
Katowice	POL	28,038	22,969	38,562,189	1,258,714	3.3%	750	915	122%
Swansea	GBR	57,374	136,243	64,088,222	171,408	0.3%	364	153	42%
Birming-ham	GBR	57,374	136,243	64,088,222	320,416	0.5%	681	287	42%

The data from Table 3 are presented as a function of the population in the selected city areas in Fig. 10. It is important to realize that the population numbers in Table 3 and Fig. 10 correspond to the city areas that were surveyed. For example, in Hamburg this was the part north of the Elbe river, not the entire city. In most cases more than 50 % of the city area was covered, making the surveys representative for that particular city. The correlation of the Marcogaz estimate with the respective urban population is very high (Fig. 10), this is not surprising as they apply a more uniform method across Europe.

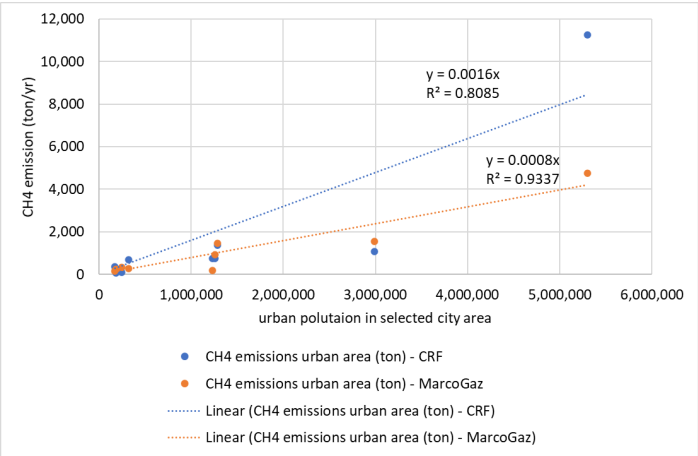

Fig. 10 Downscaled city CH_4 emissions (Table 3) as a function of population in the selected city areas for 6 countries (Note that is not representing the entire city population of the cities listed in Table 3 but only the part that was subject to MEMO² mobile campaigns).

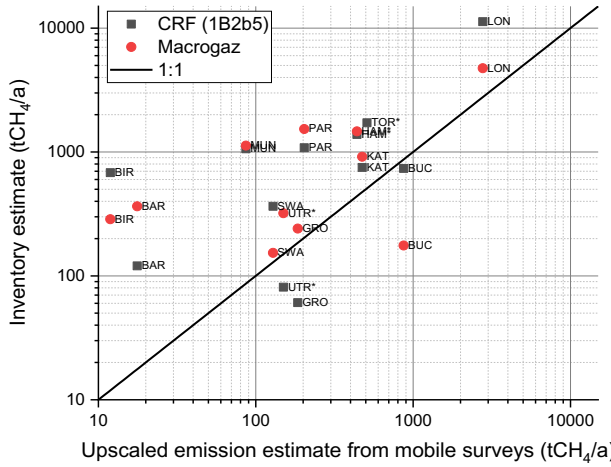

Fig. 11: Downscaled national emission inventory estimates from Marcogaz (2018) or the UNFCCC NIR CRF to the respective cities (see also Table 3) as a function of the upscaled bottom-up emission estimate from mobile (MEMO² / CCAC) surveys. Note the logarithmic scale.

The CRF based estimates uses in many case country specific emission factors and the relatively good correlation we see here is encouraging. These CRF based country specific estimates are more independent than the Marcogaz estimates but this does not imply that they are more (or less) accurate.

The measurement data collected in MEMO² give a unique opportunity to assess the new city-specific inventory estimates for different geographical regions as well as for cities of differing size, infrastructure age and socio-economic conditions. For some cities (labelled with *) in Fig. 11 emission estimates from mobile surveys were recently published (Maazallahi et al., 2020a, Pak et al., 2021). To be able to compare all cities, the data sets from all field campaigns where processed using the same approach (and code) described in Ars et al. 2020. In brief, a smooth background is fitted to the data and each CH_4 plume with an enhancement of at least 40 ppb and a width below 160 m is used to calculate an emission rate. Here, we apply the equation suggested by Weller et al. (2019), which relies on the maximum CH_4 concentration in the plume. Although this approach has limitations, due to its sensitivity to weather conditions, distance to source and intake height, using it ensures that our results are comparable to previous studies on urban natural gas CH_4 emissions in the US.

The cities included in our surveys span several orders of magnitude in terms of observed annual CH4 emissions and, in general, cities with higher inventory emissions also exhibited higher emission estimates based on our surveys. For cities on the lower end of observed emissions (10 - 100 t CH_4 / a) the inventory estimates are however, notably higher. In contrast, cities where medium emissions (100 – 1000 t CH_4 / a) were observed the inventory data is closer to the identity line. The official national inventory CRF-based approach seems less biased for this emission range. Unfortunately, only London falls into the large emission category (< 1000 t CH_4 / a) and here the Marcogaz-based estimate seems more suitable. It is important to highlight that our observation-based estimates still have significant uncertainties (> 50 %) and can be dependent on the equations used to translate observed enhancements into emission rates, but further comparison studies and controlled release experiments will improve our abilities.

3.4 Conclusion

Through MEMO² we are able to provide the first European overview of measurement-based emission estimates from natural gas distribution which can be used to confront top-down emission estimates based on the classical emission inventory approach of applying emission factors to statistical activity data. The results of this study have important similarities with the US based analysis which showed large discrepancies between cities (see Fig. 2). As was shown in section 3.3. there are significant discrepancies between two top-down estimates. Our measurement-based bottom-up approach does not agree specifically better with one of the two methods.

Hence it is a mixed message and clearly needs further analysis. For example, the results suggest that the national reported urban CH_4 emissions from the national gas distribution network is underestimated for Dutch cities and overestimated in German cities. These are interesting preliminary conclusions which will help to further improve European emission inventory data and related gridded emission maps. We need to be aware that emission inventories play an extremely important role in policy making and negations on emission reductions. Therefore, simply extrapolating our preliminary findings now to the European scale and produce new gridded emission data would be premature and could be harmful to the climate (mitigation) debate. The work done in MEMO² in this respect should be seen as an important step but not the final product that will come out of this work. This is foreseen beyond the lifetime of the project in the next 1 or 2 years when these results will be published in concord with the UNEP/CCAC programme.

4. CH_4 emissions from large festivals[3]

4.1 Overview

Next to the permanent gas distribution and supply in the urban centres there can also be temporary gas distribution and use, for example, during large festivals. Together with the Technical University of Munich, MEMO² carried out mobile measurements during the Oktoberfest in Munich, the world's largest folk festival with over 6 million visitors annually. During the 185th Oktoberfest in 2018, the use of energy added up to 2.9 million kWh of electricity and 200.937 m^3 of natural gas, 79 % of which is used for cooking and 21 % for heating (München, 2018; cited in Chen et al, 2020).

The CH_4 emissions of the 2018 Oktoberfest were measured using in situ measurements combined with a Gaussian plume dispersion model. Measurements were taken while walking and biking around the perimeter of the Oktoberfest premises (Theresienwiese) at different times of the day, during the week and at the weekend. The measured CH_4 mole fractions were plotted for each round on a map of the Oktoberfest premises to show that there is a clear correlation between the wind directions and the enhancements. Two such plots for two different wind directions are shown in Fig. 12. In addition to the concentration enhancements and the wind direction, the 16 emission sources are shown as black dots on top of each tent.

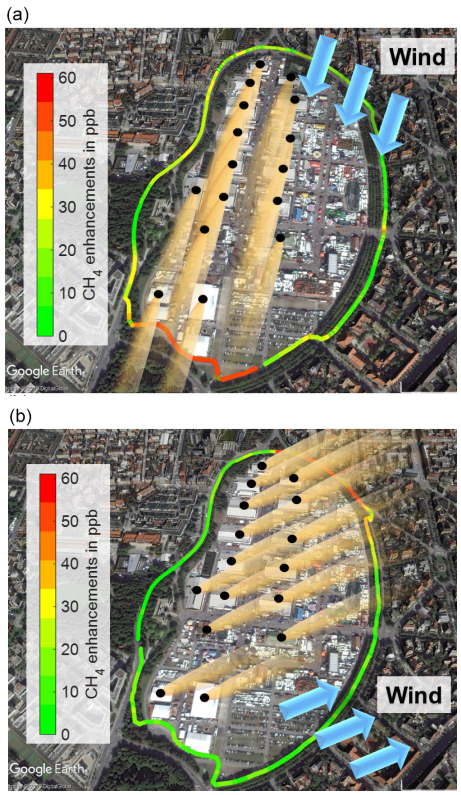

Fig. 12: CH_4 concentration enhancements of two measurement rounds including the influence of the 16 Gaussian plumes from the tents (black dots). Wind direction is (a) 20◦ and (b) −110◦. Map data: © Google, DigitalGlobe

The Gaussian plumes that are dispersed from these sources according to the measured meteorological conditions are also represented. These two plots reveal that the highest concentration enhancements can be observed downwind of the Oktoberfest premises.

[3] in collaboration with Jia Chen and Florian Dietrich, Technical University of Munich (TUM), Munich, Germany.

The average emission flux of Oktoberfest was determined as (6.7 ± 0.6) µg $m^{-2} s^{-1}$. A comparison between weekdays (4.6 µg $m^{-2} s^{-1}$) and weekend days (8.5 µg $m^{-2} s^{-1}$) shows that the emission strength at the weekend was almost twice as high compared to during the week. This correlates with a higher number of visitors during the weekend, which results in higher emissions.

During a follow-up study in 2019 the emissions were confirmed and more emphasis was placed on source attribution by using tracers (C_2H_6 and isotopes). These measurements confirmed that the emission is clearly fossil fuel based with 90 % of the emissions inside the tents coming from natural gas and only 10 % is of biogenic (human) origin. A full manuscript of this work is currently in preparation (Chen et al., manuscript in preparation, 2021).

4.1 Conclusion

The results of these investigations show that the Oktoberfest is an anthropogenic source of CH_4 that has not been accounted for in inventories until now. It was shown that the CH_4 emission was dominated by the CH_4 from fossil origin by doing isotope and ethane measurements. The studies by Chen et al. (2020, 2021) are good examples of how measurements can be used to obtain an integral flux while using additional measurements for source attribution. In this way a link can be made to the "traditional" emission inventory which builds up a complete inventory on a source by source basis. In general, it is complicated to improve an inventory if the only indication given is that the overall total may be incorrect. The inclusion of (measurement-based) source attribution is critical in this respect. The contribution of large festivals and other temporary gas use infrastructure is most likely not well represented in current emission inventories and may contribute to an underestimation of anthropogenic methane emissions in Europe. Such events should be included in future emission inventories.

5. CH_4 isotope maps based on emission inventories

5.1 Introduction

One of the ambitions of the MEMO² project was to provide gridded CH_4 isotope ($\delta^{13}C$ and $\delta^{2}H$) emissions which could be used for modelling of CH_4 concentrations and source attribution. As a first step we applied literature values to existing emissions data. At the same time MEMO² started to generate new isotope data which have bene made available through the MEMO² isotopic database which is available online (https://zenodo.org/record/4062356). The new results are described in a MEMO² deliverable by Menoud et al.[4] In this chapter we will present the MEMO² isotopic maps and make a comparison with the new MEMO² results.

5.2 CH_4 emissions

Emissions of anthropogenic origin are used from the TNO-MACC_III (Kuenen et al., 2014) and the EDGARv4.3.2 (Janssens-Maenhout et al., 2017) inventories. Natural wetland emissions are obtained from the ORCHIDEE-WET model (Ringeval et al., 2011) with a monthly time profile. The anthropogenic and wetland emissions over the European domain with a horizontal resolution of 0.5°x0.5° are illustrated in Fig. 13, and Table 4 contains the magnitude of the total and sector emissions of the inventories.

Here, CH_4 emissions are grouped into Selected Nomenclature for Air Pollution (SNAP) level-1 sectors to have a common ground for the inventories, as they use different classifications. In our European

[4] https://h2020-memo2.eu/wp-content/uploads/sites/198/2021/03/MEMO2-D2.2-v3-final.pdf

domain, agriculture (SNAP 10) is the main emitting sector, followed by the waste sector (SNAP 9). Other relevant emission sources for CH_4 are non-industrial combustion plants (SNAP 2) and the production, extraction and distribution of fossil fuels (SNAP 5). The latter two were added into one category that is named "fossil fuel related emissions" hereafter. The total anthropogenic emissions in EDGAR v4.3.2 are up to 20 % larger than in TNO-MACC_III but the relative contributions of the three main anthropogenic sectors are very similar across the inventories (Table 4).

The agriculture sector dominates (about 39 to 46 % of the total CH_4 emissions). In this sector, emissions in EDGAR v4.3.2 and TNO-MACC_III are large over Brittany in France, the BENELUX and some Eastern European countries (e.g. Romania, Belarus). For the waste sector, the differences between the inventories are largest in Eastern Europe. For the fossil fuel (FF) related emissions, large differences exist over the North Sea, Poland and the Ukraine, where the emissions in EDGAR v4.3.2 are larger than those of the TNO-MACC inventory.

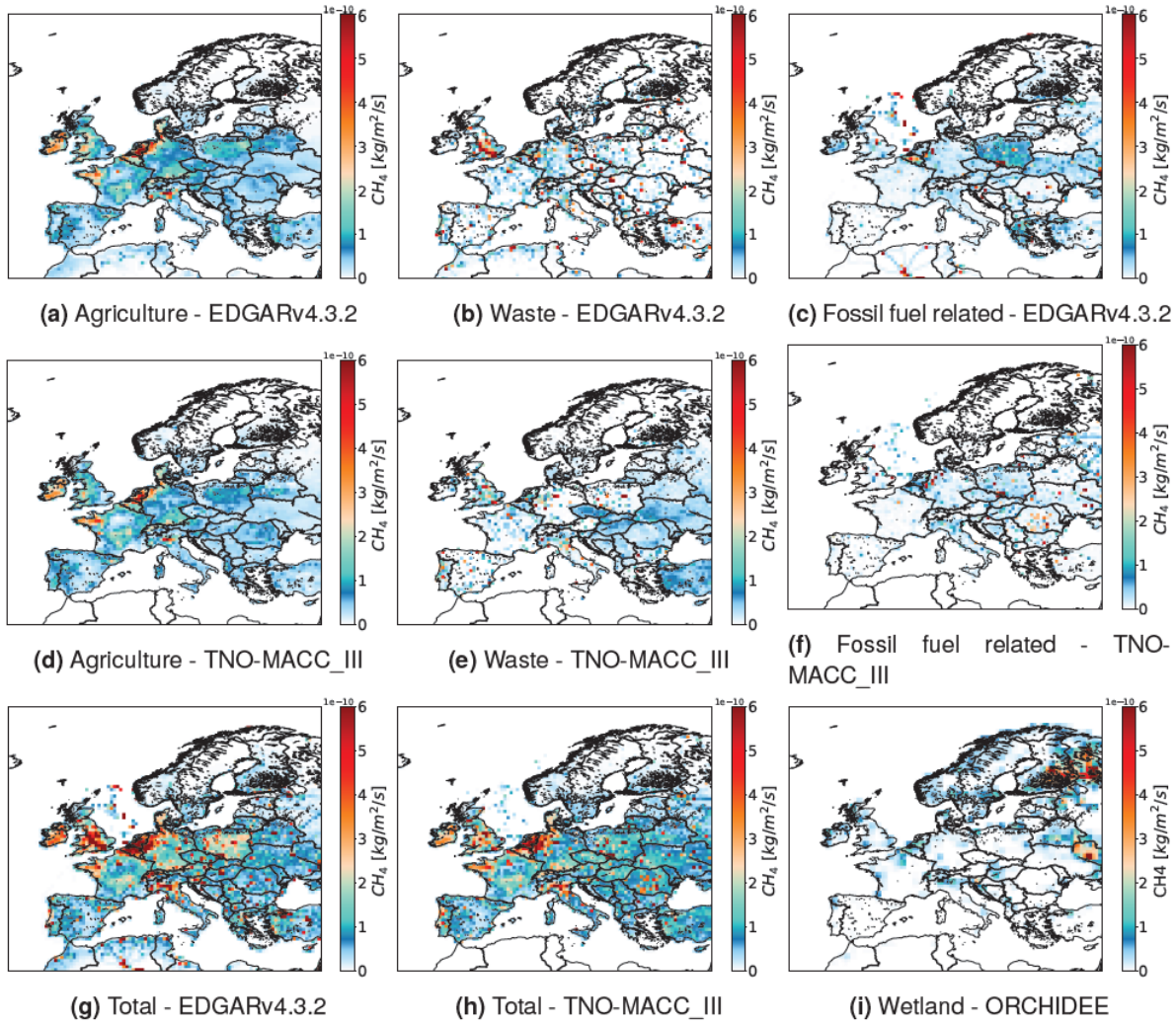

Figure 13: Anthropogenic emissions per sector (**a-f**) contributing to the total CH_4 emissions of the EDGARv4.3.2 (**g**) and TNO-MACC_III (**h**) inventory, as well as emissions from natural wetlands (**i**) obtained from the ORCHIDEE-WET model.

Table 4: Emissions [$TgCH_4/yr$] per category of the TNO-MACC_III and EDGARv4.3.2 anthropogenic as well as of natural wetlands in the full European domain. The relative contribution [%] of the sources to the total anthropogenic emissions is displayed in the column "Percentage of the total anthropogenic emissions".

SNAP code	SNAP name	Name in this study	Emissions [$TgCH_4/yr$] TNO-MACC_III	Emissions [$TgCH_4/yr$] EDGAR v4.3.2	Percentage of total anthropogenic emissions	
					TNO-MACC_III	EDGAR v4.3.2
10	Agriculture	Agriculture	10.9	12.1	24.0	23.9
9	Waste treatment and disposal	Waste	7.7	10.8	30.3	35.3
2 & 5	Non-industrial combustion plants & Distribution of fossil fuels and geothermal energy	Fossil fuel related emissions	6.1	7.3	24.0	23.9
1, 3, 4, 6, 7, 8		Other anthropogenic sources	0.7	0.4	2.8	1.3
Total anthropogenic			25.4	30.6	100.0	100.0
11	Natural emissions	Wetlands	7.8	7.8	-	-
Total			33.2	38.4		

5.3 Methane isotopic maps

Based on the main emission sectors and emission inventories used in this study, we produce maps of $\delta^{13}C$ and $\delta^{2}H$ of CH_4 sources for Europe to analyse emissions with the aid of isotopic information. Such maps provide valuable and quick insight into the source distribution and dominant source types over the domain. The $\delta^{13}C$ and $\delta^{2}H$ maps are made by using weighted emission averages of emission sectors from the inventories in combination with corresponding $\delta^{13}C$ and $\delta^{2}H$ source isotopic signatures. The applied source isotopic signatures are listed in Table 5, which are average values based on various studies, including the MEMO² deliverable D2.2 (Menoud et al., 2020b).

Table 5: Characteristic source isotopic signatures used as input for the computation of the atmospheric isotopic compositions $\delta^{13}C$ and $\delta^{2}H$, including the ranges of values found in the listed references. The $\delta^{13}C$ and $\delta^{2}H$ values for the boundary mixing ratios demonstrate the mean value as they vary over time.

Source sector	$\delta^{13}C$ [‰]	$\delta^{2}H$ [‰]	References
Agriculture (SNAP 10)	-63.5 [-74.4 – -50.3]	-306 [-442 – -168]	Menoud et al. (2020a), Sherwood et al. (2017), Levin et al. (1993), Klevenhusen et al. (2010), Bréas et al. (2001), Bilek et al. (2001), Röckmann et al. (2016), Uzaki et al. (1991), Tyler et al. (1997)
Waste (SNAP 9)	-54.9 [-73.9 – -45.4]	-290 [-347 – -172]	Bergamaschi et al. (1998), Levin et al. (1993), Zazzeri et al. (2015), Röckmann et al. (2016), Menoud et al. (2020a), Games and Hayes (1976), Sherwood et al. (2017)
Fossil fuel related emissions (SNAP 2 & 5)	-46.4 [-87.0 – -14.8]	-185 [-415 – -56]	Levin et al. (1999), Röckmann et al. (2016), Menoud et al. (2020a), Sherwood et al. (2017), Lowry et al. (2001), Thielemann et al. (2004), Zazzeri et al. (2016)
Other anthropogenic sources (SNAP 1, 3, 4, 6, 7, 8)	-38.3 [-64.4 – -12.5]	-206 [-308 – -110]	Menoud et al. (2020a), Röckmann et al. (2016), Levin et al. (1999), Chanton et al. (2000), Nakagawa et al. (2005), Sherwood et al. (2017)
Wetlands (SNAP 11)	-68.2 [-96.5 – -48.0]	-337 [-450 – -288]	Menoud et al. (2020a), Sherwood et al. (2017), Tyler et al. (1987), Smith et al. (2000), Fisher et al. (2017), Galand et al. (2010), Happell et al. (1995), Martens et al. (1992), Bilek et al. (2001), Sugimoto and Fujita (2006), Quay et al. (1999)
Boundary mixing ratios	-47.0	-86	Thanwerdas et al. (2019)

Fig. 14 shows the $\delta^{13}C$ and $\delta^{2}H$ emission maps for the European domain. Through the $\delta^{13}C$ and $\delta^{2}H$ values, a general spatial distribution of CH_4 sources is easily recognisable. The prevailing values of about -60 ‰ for $\delta^{13}C$ and -300 ‰ for $\delta^{2}H$ in both inventories indicate that CH_4 from agriculture sources dominates in Europe. In most of the capitals and larger cities (such as London, Paris), the $\delta^{13}C$ and $\delta^{2}H$ values are higher, pointing out sources connected to fossil fuels and residential combustion (e.g. heating).

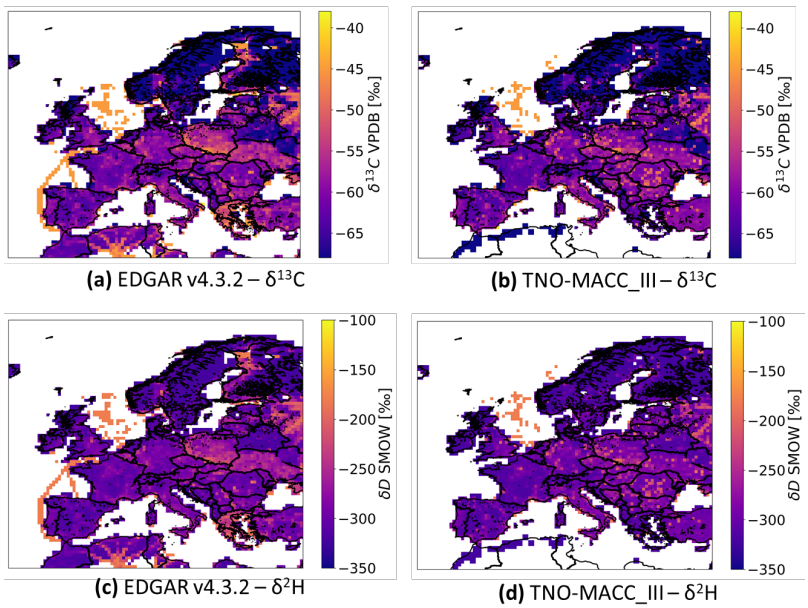

Fig. 14: Maps of $\delta^{13}C$ (top panel) and $\delta^{2}H$ (bottom panel) made from the EDGARv43.2. (left panel) and TNO-MACC_III (right panel) anthropogenic emission inventories and ORCHIDEE-WET wetland emissions as weighted average for the European domain with a horizontal resolution of 0.5°×0.5°.

Such isotopic maps highlight the differences in spatial and sector distribution of sources between the inventories (e.g. Fig. 14a and 14b).

The TNO-MACC_III inventory contains a higher ratio of FF related emissions from point sources than EDGAR, indicated by the higher $\delta^{13}C$ and $\delta^{2}H$ values in multiple single grid-cells in the TNO-MACC maps. The sources in EDGAR appear to be more diffuse, indicating a larger proportion of area sources than in TNO-MACC. This difference may be due to different definitions and treatment of point and area sources in the inventories. Another difference between the inventories is the inclusion of shipping paths in the EDGAR inventory, which are not present in the TNO-MACC inventory.

The combination of CH_4 emissions (Fig. 13) and their isotopic source signatures provide a full insight on the differences of the emission magnitudes between the inventories (Table 4). The TNO-MACC inventory includes in general more agriculture and less waste emissions than EDGAR over our European domain, which is indicated in the maps of Fig. 14 by TNO-MACC having more values below approximately -62 ‰ of $\delta^{13}C$. This is due to the agriculture sources having lower signatures assigned than waste sources (Table 4). Furthermore, EDGAR having more waste sources likely contributes to the higher $\delta^{13}C$ and $\delta^{2}H$ in larger cities where waste and FF related emissions are usually the largest sources of methane.

In order to assess the value of source isotopic signatures measured by MEMO², grid cells containing measured source isotopic signatures are replaced by the measured values and compared to the original isotopic maps shown in Fig. 14. The differences between the measured and computed isotopic values are illustrated in Fig. 15. In these maps, negative (positive) values mean that the computed source signature is lower (higher) than the measured one. The locations that appear in the maps for the two inventories differ when the locations and magnitudes of the emissions in the two inventories are different. Thus, there may be big differences between measured and computed values when using one of the inventories but none (or small and hence not visible in the map) when using the other inventory.

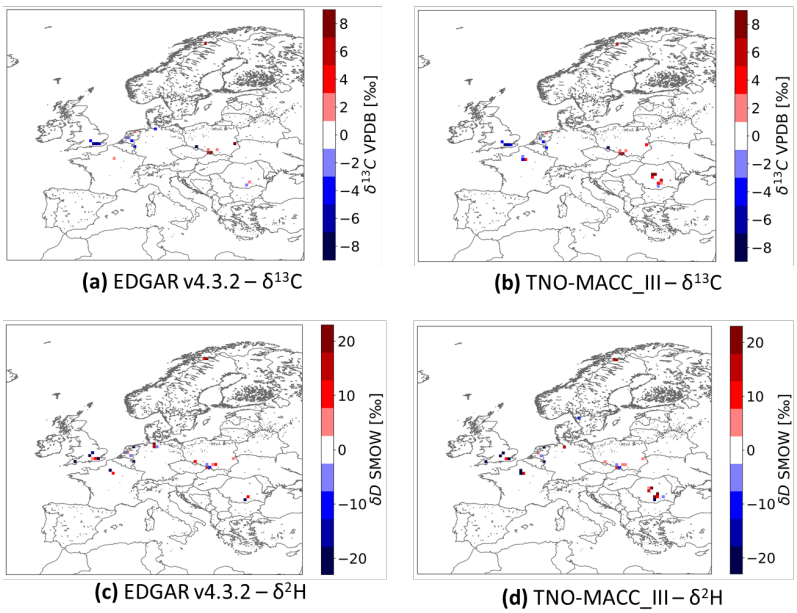

Fig. 15: Maps of $\delta^{13}C$ (top panel) and $\delta^{2}H$ (bottom panel) made from differences between measured isotopic values and isotopic values computed using the EDGARv43.2. (left panel) and TNO-MACC_III (right panel) anthropogenic emission inventories and ORCHIDEE-WET wetland emissions as weighted average for the European domain with a horizontal resolution of 0.5°×0.5°.

An example for this are the differences in Romania, where mainly CH_4 from the FF source category was measured.

When using TNO-MACC emissions as basis, measured signatures are often lower than the computed ones. This means that the applied source isotopic signature for FF related sources is not suitable for this area and that FF related emissions are not well characterised in the inventory. In contrast to this, the differences between measured and computed values are smaller when using the EDGAR inventory, which suggests that the emissions in EDGAR are closer to the measured emissions.

5.3 Discussion and outlook

This study of the isotopic composition of CH_4 gives insights into anthropogenic CH_4 emissions in inventories and how valuable measurements of CH_4 isotopologues carried out in MEMO² are, which can be used to update CH_4 emission inventories. However, while the simple method used here to compute $\delta^{13}C$ and $\delta^{2}H$ isotopic maps is useful for first assessments of emission inventories, more sophisticated methods are needed for more robust analyses. Such an analysis would be to determine average source isotopic signatures based on continuous measurement time series of ambient air, which could be used for comparisons to computed isotopic values.

Furthermore, the emission maps in Fig. 14 could be improved based on MEMO² measurements of $\delta^{13}C$ and $\delta^{2}H$ by applying the measured values of one emission type in one country to all of that country's emissions (e.g. FF emissions in Romania). However, this could introduce additional uncertainties, which need to be accounted for. Therefore, measurements of CH_4 and its isotopologues in more countries and locations are needed to gain more knowledge on CH_4 emissions in Europe and to improve CH_4 emission maps and isotopologue maps with as small uncertainties as possible.

6. Conclusion and possible impact

Current emission inventories in Europe are made by national agencies applying the classical emission inventory approach of applying emission factors to national activity data. For an explanation of this approach we refer to the Emission inventory guidebook (EEA, 2019) and Buendia et al. (2019). Recent studies, most notably in the US (e.g. Alvarez et al. 2018), have shown large discrepancies between this classical approach and measurement-based emission quantification. In MEMO² we aimed to contribute

to improved emission estimates for the European domain by doing innovative (mobile) measurements from various locations and source sectors as well as providing new isotopic measurements to support source attribution. In this report we have shown the current status and potential of improving European emission inventories using MEMO² data. It is important to acknowledge that emission inventories play an extremely important role in policy making and negotiations on emission reductions as outlined for example under the Kyoto protocol and Paris agreement. Therefore, simply extrapolating our preliminary findings to the European scale and produce new gridded emission data would be premature and could be harmful to the climate (mitigation) debate. The work done in MEMO² in this respect should be seen as an important step but not the final product that will come out of this work. A further evaluation and peer-reviewed publication of these results is needed and foreseen beyond the lifetime of the project. In the next year these results will be published in concord with the UNEP/CCAC programme. Through this channel the MEMO² results will have a substantial and lasting impact

The urban studies (chapter 3 and 4) showed that mobile measurements are capable in covering large scales of roads in urban area in quite short time and provide valuable information to attribute and quantify methane emission sources. Through MEMO² we are able to provide the first European overview of measurement-based emission estimates from natural gas distribution which can be used to confront top-down emission estimates based on the classical emission inventory approach. As was shown in section 3.3, there are significant discrepancies between two top-down estimates. Our measurement-based bottom-up approach does not agree specifically better with one of the two methods. Hence it is a mixed message and clearly needs further analysis. For example, the results suggest that the national reported urban methane emission from the national gas distribution network is underestimated for Dutch cities and overestimated in German cities. These are interesting preliminary conclusions which will help to further improve European emission inventory data and related gridded emission maps. The results can then be used for extrapolation in larger scale and also be compared to the current information in inventories. This work is ongoing and also needs interaction with for example gas distribution network operators. We have also shown that the contribution of large festivals and other temporary gas use infrastructure is most likely not well represented in current emission inventories and may contribute to an underestimation of anthropogenic methane emissions in Europe (chapter 4). Such events should be included in future emission inventories. It needs however consultation with national inventory compilers to make sure there is no double counting in the inventory.

A new approach of MEMO² was to use isotopic data connected to emission maps and by this way support source attribution. This study of the isotopic composition of CH_4 gives insights into anthropogenic CH_4 emissions in inventories and how valuable measurements of CH_4 isotopologues carried out in MEMO² are, which can be used to update CH_4 emission inventories. The isotope specific emission maps made in MEMO² can in the future be further improved based on the new MEMO² measurements of $\delta^{13}C$ and $\delta^{2}H$. Like outlined in the previous paragraph this again needs careful consideration because we have seen from the new measurements that the same source sector (especially oil and gas) can show very different isotopic signatures. Simply extrapolating our new data from limited locations to the entire European sector would only create confusion. Therefore, measurements of CH_4 and its isotopologues in more countries and locations are needed to gain more knowledge on CH_4 emissions in Europe and to improve CH_4 emission maps and isotopologue maps with as small uncertainties as possible.

8. References

Alvarez, R. A., Zavala-Araiza, D., Lyon, D. R., Allen, D. T., Barkley, Z. R., Brandt, A. R., ... & Hamburg, S. P. (2018). Assessment of methane emissions from the US oil and gas supply chain. Science, 361(6398), 186-188.

Ars, S., F. Vogel, C. Arrowsmith, S. Heerah, E. Knuckey, J. Lavoie, C. Lee, N. Mostafavi Pak, J.L. Phillips, D. Wunch, Investigation of the Spatial Distribution of Methane Sources in the Greater Toronto Area Using Mobile Gas Monitoring Systems, Environmental Science & Technology, https://dx.doi.org/10.1021/acs.est.0c05386, 2020.

Bergamaschi, P., C. Lubina, R. Königstedt, H. Fischer, A. C. Veltkamp, and O. Zwaagstra. Stable isotopic signatures (d13C, dD) of methane from European landfill sites. Journal of Geophysical Research: Atmospheres, 103(D7):8251–8265, 1998. doi: 10.1029/98JD00105. URL https://agupubs.onlinelibrary.wiley.com/doi/abs/10.1029/98JD00105.

Bilek, R. S., S. C. Tyler, M. Kurihara, and K. Yagi. Investigation of cattle methane production and emission over a 24-hour period using measurements of d13C and dD of emitted CH4 and rumen water. Journal of Geophysical Research: Atmospheres, 106(D14):15405–15413, 2001. doi: 10.1029/2001JD900177. URL https://agupubs.onlinelibrary.wiley.com/doi/abs/10.1029/2001JD900177.

Bréas, O., C. Guillou, F. Reniero, and E. Wada. The Global Methane Cycle: Isotopes and Mixing Ratios, Sources and Sinks. Isotopes in Environmental and Health Studies, 37(4):257–379, 2001. doi: 10.1080/10256010108033302. URL https://doi.org/10.1080/10256010108033302. PMID: 12723792

Bright, E. A., Coleman, P. R. and Dobson, J. E.: LandScan : A Global Population database for estimating populations at risk, [online] Available from: https://www.semanticscholar.org/paper/LandScan-%3A-A-Global-Population-database-for-at-risk-Bright-Coleman/17e6076b6761788684434d1e14e85e8877fc0146 (Accessed 23 September 2019), 2000.

Buendia, E. C., Guendehou, S., Limmeechokchai, B., Pipatti, R., Rojas, Y., Sturgiss, R., Tanabe, K., Wirth, T., Romano, D., Witi, J., Garg, A., Weitz, M. M., Cai, B., Ottinger, D. A., Dong, H., MacDonald, J. D., Ogle, S. M., Rocha, M. T., Sanchez, M. J. S., Bartram, D. M. and Towprayoon, S.: 2019 refinement to the 2006 IPCC guidelines for national greenhouse gas inventories. [online] Available from: https://www.ipcc.ch/report/2019-refinement-to-the-2006-ipcc-guidelines-for-national-greenhouse-gas-inventories/, 2019.

Chamberlain, S. D., Ingraffea, A. R. and Sparks, J. P.: Sourcing methane and carbon dioxide emissions from a small city: Influence of natural gas leakage and combustion, Environ. Pollut., 218, 102–110, doi:10.1016/J.ENVPOL.2016.08.036, 2016.

Chanton, J., C. Rutkowski, Candace Schwartz, D. Ward, and Lindsay Boring. Factors in-fluencing the stable carbon isotopic signature of methane from combustion and biomass burning. Journal of Geophysical Research, 105:1867–1877, Jan. 2000. doi: 10.1029/1999JD900909.

Chen, J., Dietrich, F., Franklin, J., Jones, T., Butz, A., Luther, A., Kleinschek, R., Hase, F., Wenig, M., Ye, S., Nouri, A., Frey, M., Knote, C., Alberti, C., and Wofsy, S.: Mesoscale Column Network for Assessing GHG and NO_x Emissions in Munich, in: Geophysical Research Abstracts, 20, EGU2018–10192–2, 2018.

Chen, J., Dietrich, F., Maazallahi, H., Forstmaier, A., Winkler, D., Hofmann, M. E. G., Denier van der Gon, H. and Röckmann, T.: Methane emissions from the Munich Oktoberfest, Atmos. Chem. Phys., 20(6), 3683–3696, doi:10.5194/acp-20-3683-2020, 2020.

EEA, EMEP/EEA air pollutant emission inventory guidebook 2019. Technical guidance to prepare national emission inventories., https://www.eea.europa.eu/publications/emep-eea-guidebook-2019 (2019)

Efron, B.: Bootstrap Methods: Another Look at the Jackknife, Ann. Stat., 7(1), 1–26, doi:10.1214/aos/1176344552, 1979.

Efron, B.: The Jackknife, the Bootstrap and Other Resampling Plans, Society for Industrial and Applied Mathematics., 1982.

Efron, B. and Tibshirani, R. J.: An Introduction to the Bootstrap - Bradley Efron, RJ Tibshirani, Champman & Hall, London. [online] Available from: https://books.google.nl/books/about/An_Introduction_to_the_Bootstrap.html?id=MWC1DwAAQBAJ&printsec=frontcover&source=kp_read_button&redir_esc=y#v=onepage&q&f=false (Accessed 4 November 2020), 1993.

Federal Environment Agency: National Inventory Report for the German Greenhouse Gas Inventory 1990 – 2017. [online] Available from: https://unfccc.int/documents/194930, 2019.

von Fischer, J. C., Cooley, D., Chamberlain, S., Gaylord, A., Griebenow, C. J., Hamburg, S. P., Salo, J., Schumacher, R., Theobald, D. and Ham, J.: Rapid, Vehicle-Based Identification of Location and Magnitude of Urban Natural Gas Pipeline Leaks, Environ. Sci. Technol., 51(7), 4091–4099, doi:10.1021/acs.est.6b06095, 2017.

Fisher, R. J. France, David Lowry, Mathias Lanoisellé, Rebecca Brownlow, John Pyle, Michelle Cain, Nicola Warwick, U. Skiba, Julia Drewer, Kerry Dinsmore, Sarah Leeson, Stéphane Bauguitte, Axel Wellpott, Sebastian O'Shea, Grant Allen, Martin Gallagher, Joseph Pitt, Carl Percival, and Euan Nisbet. Measurement of the 13C isotopic signature of methane emissions from northern European wetlands. Global Biogeochemical Cycles, 31, Mar. 2017. doi: 10.1002/2016GB005504.

Galand P., Kim Yrjälä, and R. Conrad. Stable carbon isotope fractionation during methanogenesis in three boreal peatland ecosystems. Biogeosciences, 7, Nov. 2010. doi: 10.5194/bg-7-3893-2010.

Gallagher, M. E., Down, A., Ackley, R. C., Zhao, K., Phillips, N. and Jackson, R. B.: Natural Gas Pipeline Replacement Programs Reduce Methane Leaks and Improve Consumer Safety, Environ. Sci. Technol. Lett., 2(10), 286–291, doi:10.1021/acs.estlett.5b00213, 2015.

Games, L. M. and J. M. Hayes. On the mechanisms of CO2 and CH4 production in natural anaerobic environments. Environmental Biogeochemistry, pages 51–73, 1976.

Gioli, B., Toscano, P., Lugato, E., Matese, A., Miglietta, F., Zaldei, A. and Vaccari, F. P.: Methane and carbon dioxide fluxes and source partitioning in urban areas: The case study of Florence, Italy, Environ. Pollut., 164, 125–131, doi:10.1016/j.envpol.2012.01.019, 2012.

Happell, J. D., Jeffrey P. Chanton, and William J. Showers. Methane transfer across the water-air interface in stagnant wooded swamps of Florida: Evaluation of mass-transfer coefficients and isotropic fractionation. Limnology and Oceanography, 40(2):290–298, 1995. doi: 10.4319/lo.1995.40.2.0290. URL https://aslopubs.onlinelibrary.wiley.com/doi/abs/10.4319/lo.1995.40.2.0290.

Helfter, C., Tremper, A. H., Halios, C. H., Kotthaus, S., Bjorkegren, A., Sue, C., Grimmond, B., Barlow, J. F. and Nemitz, E.: Spatial and temporal variability of urban fluxes of methane, carbon monoxide and carbon dioxide above London, UK, Atmos. Chem. Phys, 16, 10543–10557, doi:10.5194/acp-16-10543-2016, 2016.

Hendrick, M. F., Ackley, R., Sanaie-Movahed, B., Tang, X. and Phillips, N. G.: Fugitive methane emissions from leak-prone natural gas distribution infrastructure in urban environments, Environ. Pollut., 213, 710–716, doi:10.1016/j.envpol.2016.01.094, 2016.

Hopkins, F. M., Kort, E. A., Bush, S. E., Ehleringer, J. R., Lai, C.-T., Blake, D. R. and Randerson, J. T.: Spatial patterns and source attribution of urban methane in the Los Angeles Basin, J. Geophys. Res. Atmos., 121(5), 2490–2507, doi:10.1002/2015JD024429, 2016.

Hu, N., Liu, S., Gao, Y., Xu, J., Zhang, X., Zhang, Z. and Lee, X.: Large methane emissions from natural gas vehicles in Chinese cities, Atmos. Environ., 187, 374–380, doi:10.1016/j.atmosenv.2018.06.007, 2018.

Jackson, R. B., Down, A., Phillips, N. G., Ackley, R. C., Cook, C. W., Plata, D. L. and Zhao, K.: Natural gas pipeline leaks across Washington, DC, Environ. Sci. Technol., 48(3), 2051–2058, doi:10.1021/es404474x, 2014.

Janssens-Maenhout, G., M. Crippa, D. Guizzardi, M. Muntean, E. Schaaf, F. Dentener, P. Bergamaschi, V. Pagliari, J. G. J. Olivier, J. A. H. W. Peters, J. A. van Aardenne, S. Monni, U. Doering, and A. M. R. Petrescu. EDGAR v4.3.2 Global Atlas of the three major Greenhouse Gas Emissions for the period 1970–2012. Earth System Science Data Discussions, 2017:1–55, 2017. doi: 10.5194/essd-2017-79. URL https://www.earth-syst-sci-data-discuss.net/essd-2017-79/.

Keeling, C. D.: The concentration and isotopic abundances of atmospheric carbon dioxide in rural areas, Geochim. Cosmochim. Acta, 13(4), 322–334, doi:10.1016/0016-7037(58)90033-4, 1958.

Keeling, C. D.: The concentration and isotopic abundances of carbon dioxide in rural and marine air, Geochim. Cosmochim. Acta, 24(3–4), 277–298, doi:10.1016/0016-7037(61)90023-0, 1961.

Klevenhusen, F., Stefano Bernasconi, M Kreuzer, and Carla Soliva. Experimental validation of the Intergovernmental Panel on Climate Change default values for ruminant-derived methane

Lamb, B. K., Cambaliza, M. O. L., Davis, K. J., Edburg, S. L., Ferrara, T. W., Floerchinger, C., Heimburger, A. M. F., Herndon, S., Lauvaux, T., Lavoie, T., Lyon, D. R., Miles, N., Prasad, K. R., Richardson, S., Roscioli, J. R., Salmon, O. E., Shepson, P. B., Stirm, B. H. and Whetstone, J.: Direct and Indirect Measurements and Modeling of Methane Emissions in Indianapolis, Indiana, Environ. Sci. Technol., 50(16), 8910–8917, doi:10.1021/acs.est.6b01198, 2016.

Lebel, E. D., Lu, H. S., Speizer, S. A., Finnegan, C. J. and Jackson, R. B.: Quantifying Methane Emissions from Natural Gas Water Heaters, Environ. Sci. Technol., 54(9), 5737–5745, doi:10.1021/acs.est.9b07189, 2020.

Maazallahi, H., Fernandez, J. M., Menoud, M., Zavala-Araiza, D., Weller, Z. D., Schwietzke, S., von Fischer, J. C., Denier van der Gon, H., and Röckmann, T.: Methane mapping, emission quantification, and attribution in two European cities: Utrecht (NL) and Hamburg (DE), Atmos. Chem. Phys., 20, 14717–14740, https://doi.org/10.5194/acp-20-14717-2020, 2020a.

Maazallahi, H., Fernandez, J. M., Menoud, M., Zavala-Araiza, D., Weller, Z. D., Schwietzke, S., von Fischer, J. C., Denier van der Gon, H. and Röckmann, T.: MATLAB code for evaluation of Urban Surveys, , doi:10.5281/zenodo.3928972, 2020b.

McKain, K., Down, A., Raciti, S. M., Budney, J., Hutyra, L. R., Floerchinger, C., Herndon, S. C., Nehrkorn, T., Zahniser, M. S., Jackson, R. B., Phillips, N. and Wofsy, S. C.: Methane emissions from natural gas infrastructure and use in the urban region of Boston, Massachusetts, Proc. Natl. Acad. Sci., 112(7), 1941–1946, doi:10.1073/PNAS.1416261112, 2015.

München: Oktoberfest 2018 Schlussbericht, available at: https://www.ris-muenchen.de/RII/RII/DOK/SITZUNGSVORLAGE/5440803.pdf (last access: 13 March 2020), 2018.

muenchen.de: Oktoberfest-Barometer: Die beste Zeit für den Wiesnbesuch, available at: https://www.muenchen.de/veranstaltungen/oktoberfest/besucher-service/wiesnbarometer.html (last access: 9 July 2019), 2018.

Nam, E. K., T. E. Jensen, A. and Wallington, T. J.: Methane Emissions from Vehicles, Environ. Sci. Technol., doi:10.1021/ES034837G, 2004.

Naus, S., Röckmann, T. and Popa, M. E.: The isotopic composition of CO in vehicle exhaust, Atmos. Environ., 177, 132–142, doi:10.1016/J.ATMOSENV.2018.01.015, 2018.

O'Shea, S. J., Allen, G., Fleming, Z. L., Bauguitte, S. J.-B., Percival, C. J., Gallagher, M. W., Lee, J., Helfter, C. and Nemitz, E.: Area fluxes of carbon dioxide, methane, and carbon monoxide derived from airborne measurements around Greater London: A case study during summer 2012, J. Geophys. Res. Atmos., 119(8), 4940–4952, doi:10.1002/2013JD021269, 2014.

Pak, N. M., Heerah, S., Zhang, J., Chan, E., Worthy, D., Vogel, F., & Wunch, D. (2021). The Facility Level and Area Methane Emissions inventory for the Greater Toronto Area (FLAME-GTA). Atmospheric Environment, 252, 118319.

Peek, C. J., Montfoort, J. A., Dröge, R., Guis, B., Baas, K., Huet, B. van, Hunnik, O. R. van and Berghe, A. C. W. M. van den: Methodology report on the calculation of emissions to air from the sectors Energy, Industry and Waste, as used by the Dutch Pollutant Release and Transfer Register., 2019.

Phillips, N. G., Ackley, R., Crosson, E. R., Down, A., Hutyra, L. R., Brondfield, M., Karr, J. D., Zhao, K. and Jackson, R. B.: Mapping urban pipeline leaks: Methane leaks across Boston, Environ. Pollut., 173, 1–4, doi:10.1016/j.envpol.2012.11.003, 2013.

Popa, M. E., Vollmer, M. K., Jordan, A., Brand, W. A., Pathirana, S. L., Rothe, M. and Röckmann, T.: Vehicle emissions of greenhouse gases and related tracers from a tunnel study: CO : CO2 , N2O : CO2 , CH4 : CO2 , O2 : CO2 ratios, and the stable isotopes 13C and 18O in CO2 and CO, Atmos. Chem. Phys., 14(4), 2105–2123, doi:10.5194/acp-14-2105-2014, 2014.

Tong, L. I., Chang, C. W., Jin, S. E. and Saminathan, R.: Quantifying uncertainty of emission estimates in National Greenhouse Gas Inventories using bootstrap confidence intervals, Atmos. Environ., 56, 80–87, doi:10.1016/j.atmosenv.2012.03.063, 2012.

U.S. EIA: Natural gas consumptions in the United States, [online] Available from: https://www.eia.gov/energyexplained/natural-gas/use-of-natural-gas.php (Accessed 16 June 2020), 2019.

US Census Bureau: U.S. and World Population Clock, [online] Available from: https://www.census.gov/popclock/ (Accessed 20 June 2020), 2020.

Weller, Z., Hamburg, S. P. and von Fischer, J. C.: A national estimate of methane leakage from pipeline mains in natural gas local distribution systems, Environ. Sci. Technol., doi:10.1021/acs.est.0c00437, 2020.

Weller, Z. D., Roscioli, J. R., Daube, W. C., Lamb, B. K., Ferrara, T. W., Brewer, P. E. and von Fischer, J. C.: Vehicle-Based Methane Surveys for Finding Natural Gas Leaks and Estimating Their Size: Validation and Uncertainty, Environ. Sci. Technol., acs.est.8b03135, doi:10.1021/acs.est.8b03135, 2018.

Weller, Z. D., Yang, D. K. and von Fischer, J. C.: An open source algorithm to detect natural gas leaks from mobile methane survey data, edited by M. Mauder, PLoS One, 14(2), e0212287, doi:10.1371/journal.pone.0212287, 2019.

Yacovitch, T. I., Herndon, S. C., Roscioli, J. R., Floerchinger, C., McGovern, R. M., Agnese, M., Pétron, G., Kofler, J., Sweeney, C., Karion, A., Conley, S. A., Kort, E. A., Nähle, L., Fischer, M., Hildebrandt, L., Koeth, J., McManus, J. B., Nelson, D. D., Zahniser, M. S. and Kolb, C. E.: Demonstration of an Ethane Spectrometer for Methane Source Identification, Environ. Sci. Technol., 48(14), 8028–8034, doi:10.1021/es501475q, 2014.

Zimnoch, M., Necki, J., Chmura, L., Jasek, A., Jelen, D., Galkowski, M., Kuc, T., Gorczyca, Z., Bartyzel, J. and Rozanski, K.: Quantification of carbon dioxide and methane emissions in urban areas: source apportionment based on atmospheric observations, Mitig. Adapt. Strateg. Glob. Chang., 24(6), 1051–1071, doi:10.1007/s11027-018-9821-0, 2019.